Quaternary Science Reviews 220 (2019) 178–187

Contents lists available at ScienceDirect

Quaternary Science Reviews

journal homepage: www.elsevier.com/locate/quascirev

Holocene glacier fluctuations in Patagonia are modulated by summer insolation intensity and paced by Southern Annular Mode-like variability

Scott A. Reynhout [a, b], Esteban A. Sagredo [b, c, *], Michael R. Kaplan [d, e], Juan Carlos Aravena [e], Mateo A. Martini [f], Patricio I. Moreno [b, g], Maisa Rojas [b, h, j], Roseanne Schwartz [d], Joerg M. Schaefer [d, i]

[a] Departamento de Geología, Facultad de Ciencias Físicas y Matemáticas, Universidad de Chile, Plaza Ercilla 803, 8370450 Santiago, Chile
[b] Núcleo Milenio Paleoclima, Universidad de Chile, Las Palmeras 3425, Ñuñoa, Chile
[c] Instituto de Geografía, Pontificia Universidad Católica de Chile, Avenida Vicuña Mackenna 4860, 7820436 Macul, Chile
[d] Lamont-Doherty Earth Observatory, P.O. Box 1000, 61 Route 9W, Palisades, NY 10964-100, USA
[e] Centro de Investigación Gaia Antártica, Universidad de Magallanes, Avenida Bulnes 01855, 62000009, Punta Arenas, Chile
[f] Centro de Investigaciones en Ciencias de la Tierra (CONICET-Facultad de Ciencias Exactas, Físicas y Naturales, UNC), Vélez Sársfeld 1611, X5016GCA, Córdoba, Argentina
[g] Departamento de Ciencias Ecológicas, Facultad de Ciencias, Universidad de Chile, Las Palmeras 3425, Ñuñoa, Chile
[h] Departamento de Geofísica, Facultad de Ciencias Físicas y Matemáticas, Universidad de Chile, Avenida Blanco Encalada 2002, Santiago, Chile
[i] Department of Earth and Environmental Sciences of Columbia University, New York, NY, 10027, USA
[j] Center for Climate and Resilience Research (CR2), Blanco Encalada 2002, Santiago, Chile

ARTICLE INFO

Article history:
Received 28 January 2019
Received in revised form
27 May 2019
Accepted 30 May 2019

Keywords:
Holocene
Glaciation
Paleoclimatology
South America
Cosmogenic isotopes
Geomorphology
Glacial
Insolation
Southern annular mode

ABSTRACT

Alpine glaciers are sensitive indicators of changes in climate, and their ubiquity in mountainous regions make them valuable proxies for terrestrial climate reconstructions worldwide. However, the timing and extent of glacier change across the South American mid-latitudes through the Holocene are still poorly constrained relative to their counterparts in the Northern Hemisphere. Here we report a new ^{10}Be surface exposure-based chronology of moraines recording a series of progressively less-extensive glacier advances of Glaciar Torre (Argentina, 49.3°S/73.0°W) since the Last Glacial Maximum, with expansions culminating at 17,600 ± 900, 13,500 ± 500, 9700 ± 400, 6900 ± 200, 6100 ± 300, 4500 ± 200, and 530 ± 60 yr BP. The declining magnitude of Holocene glacier expansions parallels a gradual rise in local summer insolation intensity during the Holocene, while individual advances occurred during inferred negative Southern Annular Mode (SAM)-like states at centennial to millennial timescales. These observations suggest that (i) summer insolation intensity modulated antiphased trends in glacier extent in the polar hemispheres during the Holocene, and that (ii) centennial-scale 'SAM-like' temperature and precipitation anomalies paced glacier fluctuations throughout Patagonia. Given the persistence of the inferred 'SAM-like' anomalies throughout the Holocene, the modern measured trend towards positive SAM index conditions could mark the onset of a fundamental shift in the climate of the Southern Hemisphere midlatitudes that warrants consideration in projections of future climate.

1. Introduction

At least five decades of studies on glaciers around the North Atlantic sector have revealed a general pattern of progressively larger glacier expansions during the Holocene, culminating in glacier maxima within the last 600 years (Porter and Denton, 1967; Denton and Karlén, 1973; Ivy-Ochs et al., 2009; Nesje, 2009; Carlson et al., 2014). As alpine glaciers respond to decadal-to millennial-scale climate change (Mackintosh et al., 2017), this pattern has been interpreted to support a warm early-to middle-Holocene, although some glaciers did expand during this period (Nesje, 2009; Schimmelpfennig et al., 2012). Several explanations have been

* Corresponding author. Núcleo Milenio Paleoclima, Universidad de Chile, Las Palmeras 3425, Ñuñoa, Chile.
E-mail address: esagredo@uc.cl (E.A. Sagredo).

https://doi.org/10.1016/j.quascirev.2019.05.029
0277-3791/

proposed for this pattern in Europe and North America; however, if the opposing trend of progressively smaller glacier advances during the Holocene in New Zealand (Schaefer et al., 2009; Putnam et al., 2012; Kaplan et al., 2013) represents a Southern Hemisphere-wide pattern, antiphased trends in summer insolation intensity between the Northern and Southern Hemispheres may be implicated as a 'modulator' of global mid-latitude glacier extent.

Paleoglacier studies in southern Patagonia (defined here as South America between 46° and 53°S) reveal a glacial chronology different from those in New Zealand and the Northern Hemisphere. Several models of "Neoglaciation" have been proposed, often dissimilar from each other, although all suggest that an early Holocene warm period was followed immediately by mid-Holocene glacier maxima and progressively smaller glaciations in the mid-to late-Holocene (Mercer, 1965; Clapperton and Sugden, 1988; Glasser et al., 2004; Aniya, 2013; Strelin et al., 2014; Kaplan et al., 2016). Although this pattern differs from the progressively less- and more-extensive Holocene glaciations in New Zealand and the Northern Hemisphere, respectively, early workers (Porter and Denton, 1967; Mercer, 1982) drew implicit parallels across the polar hemispheres by defining the Patagonian record in terms of a warm "Hypsithermal" followed by a colder "Neoglacial" period (Porter, 2000). The failure of present glacier chronologies to identify coherent hemispheric trends in climate colors our understanding of Holocene climate and suggests no single factor has governed glacier behavior over this time period (Solomina et al., 2015).

An important caveat in Patagonian glacier studies is the continued reliance on chronologies based on minimum-limiting age dating. Kaplan et al. (2016) note that, until recently, most prior studies had to rely on minimum ages to constrain Holocene glacier advances or retreats. A common method involves radiocarbon dating of organic matter overlying glacial deposits. This method yields valid results when interpreted as minimum-limiting ages of a geologic event; however, a key assumption for the use of these data to constrain Holocene climate variability is that the time lag between deposition and colonization by vegetation is minimal. Lags of centuries to millennia—or periods of erosion between initial and subsequent colonization—can result in valid limiting ages of low precision. New age constraints of previously dated moraines in Patagonia have demonstrated that the original minimum-limiting ages often underestimated the true age of the landform by thousands of years, for instance at Peninsula Herminita (Aniya and Sato, 1995; Strelin et al., 2011; Kaplan et al., 2016), Lago Pearson (Mercer, 1965; Kaplan et al., 2016), and at Glaciar Frías (Mercer, 1976; Strelin et al., 2014; Kaplan et al., 2016).

We stress that the original ages reported in such sites are not incorrect; the actual ages of the dated moraines predate the originally-reported ages, which is consistent with the *a priori* implications of minimum-limiting ages. However, the existing models of Holocene glaciation in Patagonia were constructed in part assuming that minimum-limiting ages served as close (e.g. sub-millennial) approximations of the true age of a glacial advance. As multiple studies have now demonstrated that this assumption cannot be universally sustained in this region, a reevaluation of the preexisting Holocene glacier chronology is necessary to evaluate sub-millennial climate variability.

We set out to improve our understanding of the timing and extent of Patagonian glacier fluctuations since the Last Glacial Maximum (LGM) by developing a new ^{10}Be chronology for a sequence of well-preserved moraines deposited by Glaciar Torre in southwestern Patagonia. Using this chronology, we evaluate the regional coherence between published glacier chronologies, the putative role of summer insolation intensity in mid-latitude glacier fluctuations (Kaufman et al., 2004) throughout the Southern Hemisphere, and a suggested link between distinct glacier expansions and quasi-modern climate variability at centennial timescales during the Holocene.

2. Study area

2.1. Setting

Glaciar Torre (~50 km^2, 49.32°S/73.02°W) is located approximately 20 km north of Glaciar Viedma, the eastern outlet of the Southern Patagonian Icefield (SPI) into Lago Viedma (Fig. 1a). Glaciar Torre lies adjacent to, but is independent from the Icefield, separated to the west by a >500 m headwall formed by the Cerro Torre chain of peaks. Lliboutry (1953) identifies the glacier as a compound glacier composed of three tributary ice bodies named Adela, Grande, and Torre; it is sometimes erroneously referred to as the Fitz Roy glacier. We follow the convention established by Masiokas et al. (2009) by referring to the entire glacier system as Glaciar Torre, although the bulk of the present glacier front consists of ice originating from Glaciar Adela. The glacier terminates in an ice-marginal lake (Laguna Torre; Fig. 1c), which formed as ice retreated from the innermost moraine M7. Ice was land-terminating when the moraines we focus on ("M0"-M7) were formed, as evidenced by the extensive system of terminal moraines, meltwater channels, and outwash deposits associated with past glacier highstands (Fig. 1b).

The chronologic potential within the well-preserved series of end moraines of the Torre Glacier system (Fig. 1b) has been recognized for over 60 years (Heim, 1951; Auer, 1956; Lawrence and Lawrence, 1959; Mercer, 1965). However, few studies have been carried out to evaluate the absolute ages of these landforms. Mercer (1965) provided one minimum-limiting radiocarbon age for the "Fitz Roy III moraine" (M3) of 800 ± 85 ^{14}C yr for a basal peat behind the moraine, and a dendrochronologically-derived minimum-limiting age of ~1695 CE for the "outer Fitz Roy IV moraine" (M4). Masiokas et al. (2009) used dendrochronologic surface exposure dating to estimate "Little Ice Age" minimum-limiting ages for moraines M3-M7 but were unable to obtain limiting ages for the older moraines. This chronology formed the basis of a regional *Rhizocarpon* calibration curve (Garibotti and Villalba, 2009), which suggests latest-Holocene ages for all moraines identified in the area.

2.2. Regional climatology

Regional climate is characterized by the dominant influence of the Southern Westerly Winds (SWW) and the orographic forcing imposed by the Patagonian Andes, resulting in a pronounced west-east gradient in several climatic variables. Precipitation reaches Patagonia in the form of westerly frontal systems guided by the upper-level jet, which is largely symmetric across the southern hemisphere (Garreaud et al., 2009). Precipitation varies from up to 10,000 mm/yr west of the Andean divide to less than 300 mm/yr to the east; zonal westerly flow correlates positively (negatively) with precipitation to the west (east) of the divide, consistent with the development of a strong rain-shadow effect (Garreaud et al., 2013). This longitudinal transition is also seen in the progressive increase of incoming solar radiation towards the east (Schaefer et al., 2015) and the sharp transition in vegetation within the study area. From west to east, the dominant ecoregion transitions from polar ice cap conditions near the eastern limit of the SPI, to a narrow belt of Subantarctic evergreen and deciduous forest, to Patagonian steppe, in less than 20 km (Olson et al., 2001).

Meteorological station data are sparse in the region, but the few stations that exist near the limits of the SPI exhibit historical mean annual temperatures of ~6 °C (Miller, 1976; Carrasco et al., 2002). A long-term warming trend is apparent across southern Patagonia

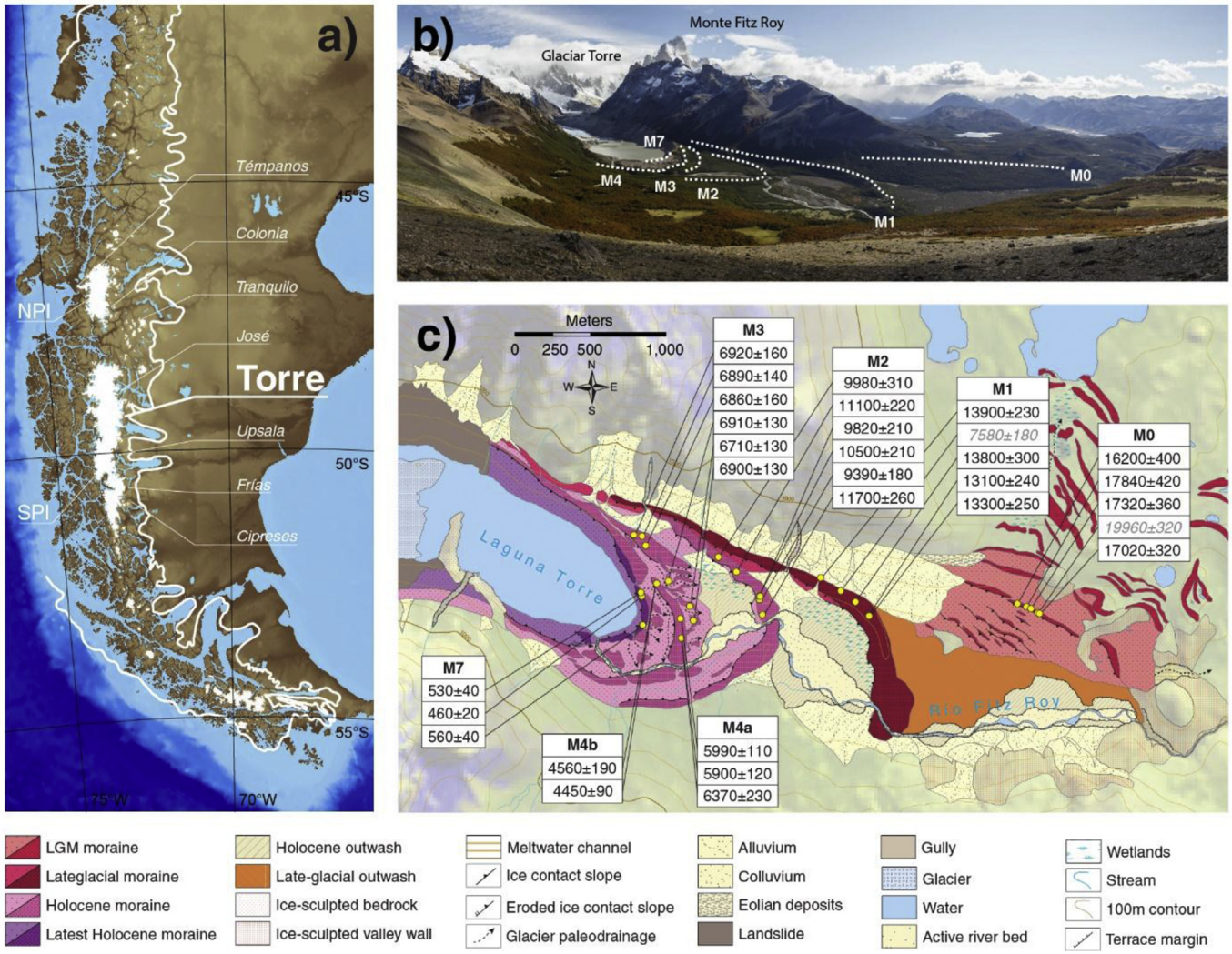

Fig. 1. a) Regional overview with sites mentioned in this paper. White areas represent present ice cover and the white line shows LGM ice extent. SPI = Southern Patagonian Icefield, NPI = Northern Patagonian Icefield. b) Photo of the study area, emphasis on moraine ridge crests. View to the north. c) Glacial geomorphology of the study area and ^{10}Be ages (±1σ internal error) for each dated moraine (yr BP). Ages in gray italics indicate outliers excluded from discussion (see Supplementary Information).

over the 20th century, driven primarily by increases in summer (DJF) temperatures (Villalba et al., 2003). West of the orographic divide, trends in precipitation reflect southerly intensification of the SWW during this period, with a 300–800 mm decade^{-1} decline north of 50°S and a 200–300 mm decade^{-1} increase south of 50°S from 1978 to 2001; east of the divide trends are insignificant (Garreaud et al., 2013). Regional surface energy mass balance modeling of the SPI suggests that increased orographic precipitation—linked with SWW intensification—could have resulted in modelled positive mass balance over the period of 1975–2011 (Schaefer et al., 2015). However, this same study indicates that during this period Glaciar Torre experienced net negative mass balance, incongruent with an increase in precipitation. The negative mass balance trend is better explained as a response to warmer temperatures over the last several decades (Rignot et al., 2003; Rivera and Casassa, 2004; Rasmussen et al., 2007).

Observations of elevated temperatures and a poleward shift and intensification of the SWW are consistent with recent persistently positive phases of the Southern Annular Mode/Antarctic Oscillation (SAM/AAO; hereafter SAM). The SAM is a mode of climatic variability associated with summer (DJF) intensification of the SWW over the Southern Ocean during the latter half of the 20th century (Jones et al., 2016). Positive (negative) phases of the SAM reflect poleward (equatorward) shifts and strengthening (weakening) of the SWW and Antarctic polar vortex, leading to warmer (colder) conditions in Patagonia and increased (decreased) orographic precipitation west of the orographic divide (Gillett et al., 2006; Garreaud et al., 2009; Thompson et al., 2011; Villalba et al., 2012). Registries of the SAM beyond instrumental records indicate multidecadal to centennial trends over the past millennium (Villalba et al., 2012; Abram et al., 2014), and suggest SAM-like variability has existed at centennial timescales through the Holocene (Moreno et al., 2018).

3. Methods

Mapping of glacial landforms enabled us to identify eight well-preserved moraine complexes distal to the modern ice margin of Glaciar Torre (Fig. 1b). These moraines are sharp-crested, variably dissected by paleochannels or modern drainages, with slope angles in the sampled areas below the angle of repose of unconsolidated sediment. Following prior convention (Masiokas et al., 2009), we

label them M0 to M7 in ascending chronostratigraphic order. From these latero-frontal moraines, we collected 30 samples from boulders to establish the age of at least six glacier expansions (Fig. 1c).

Rock samples were taken for ^{10}Be surface exposure dating from large (>1 m^3) boulders rooted in the crests of moraine ridges (Fig. S1). An assumption underlying this method is that boulders deposited at this position were deposited during the final phases of a glacier advance, and their exposure ages will reflect the age of moraine stabilization following glacier retreat. We assume that we sample the final part of the moraine constructed (i.e. the top) and that moraine stabilization occurred immediately after the withdrawal of Glaciar Torre from the moraine-forming position. We also assume advance and retreat of Glaciar Torre was primarily a function of climate; Sagredo et al. (2014) suggested that southern Patagonian glaciers are relatively more sensitive to variations in temperature than precipitation, due to the region's shallower atmospheric lapse rate and greater atmospheric emissivity. We therefore assume the age of moraine stabilization therefore closely dates the inflection point when local climatic conditions—specifically temperature—changed from favorable to unfavorable for glacier advance. Strictly speaking, our moraine ages are considered close minimum-limiting ages marking the end of glacial expansions.

Rhyodacitic and granodioritic lithologies were sampled; total sample quartz content varied between 5 and 35%. Samples >0.5 m tall were preferentially sampled to avoid possible effects of burial and posterior exhumation of boulders. Sampling taller boulders also reduces the likelihood of long-term burial under thick snow, the impact of which we consider minor and for which we do not correct. Rock surfaces presenting few signs of surficial pitting or erosion were preferentially selected, avoiding any surfaces that show obvious signs of erosion (e.g. spalling, flaking), although the effects of *in situ* weathering are assumed to be negligible due to the young age of the samples. We therefore do not correct for erosion in our age calculations. Samples were taken from the top 1–4 cm of planar to gently curved non-vegetated surfaces using a drill and explosive charges. A topographic skyline, as well as surficial strike and dip measurements, were made using a pocket transit and clinometer for shielding corrections. Coordinates and altitude were evaluated relative to the WGS 1984 datum using a handheld commercial GPS with an assumed uncertainty of 5 m in the horizontal plane and 5-10 m in the vertical.

Initial rock crushing took place at the Pontificia Universidad Católica de Chile; mineral separation, beryllium isolation, and final sample preparation occurred at the Cosmogenic Nuclide Laboratory at Lamont-Doherty Earth Observatory following established geochemical protocols (Schaefer et al., 2009; Kaplan et al., 2011). Dating of latest-Holocene boulders is made possible only through recent advances in cosmogenic dating techniques that permit analysis of very low ^{10}Be/^{9}Be ratios (~10^{-16}). The two critical components are 1) the low process blank utilized at the Lamont cosmogenic nuclide laboratory, and 2) a custom ion source utilized for AMS measurements at the Center for Accelerator Mass Spectrometry at Lawrence Livermore National Laboratory. Analytical data are available in Table 1.

^{10}Be ages were calculated based on methods incorporated in the CRONUS-Earth online exposure age calculators (v. 2.2) (Balco et al., 2008), using the time-dependent Lal/Stone scaling model and the regional Patagonian production rate (Kaplan et al., 2011). We report mean moraine ages with the propagation of the analytical uncertainty and local production rate uncertainties (3%) (Kaplan et al., 2011) for comparison with other proxy records. We base our discussion on ages using version 2.2.1 of the constants file, as it is modified with a high-resolution version of the geomagnetic framework (Lifton et al., 2008) to be consistent with calculations made by Kaplan et al. (2011). Our choice of constants file and scaling model does not fundamentally alter our conclusions (see Table S1). Radiocarbon ages presented in the discussion were calculated as cal yr BP using the SHCal13 calibration (Hogg et al., 2013) and CALIB v. 7.0.4 (Stuiver and Reimer, 2018).

4. Results

Six of the eight identified moraine crests in the study area were dated. Moraine ages, along with summary statistics, are presented as summed probability distributions in Figs. S2 and S3. Analytical data pertinent to the computation of ages are presented in Table 1; Table S2 presents individual ages according to different production rate scaling schemes. Geomorphologic interpretations, along with a discussion of outliers, are presented below.

4.1. Moraine M0: 17,100 ± 860 yr BP (n = 4, 1 outlier excluded)

M0 is a relatively small (max. 10 m tall) lateral moraine crest preserved in dense forest on the north slope of the Fitz Roy valley. Five samples were taken from boulders astride the ~10 m ridge crest of M0. Greater evidence of superficial pitting and flaking was evident on the granitic boulders that comprise these samples, which suggest that weathering may have affected them to a greater degree; this would have the net effect of reducing the perceived age of these boulders, suggesting the average age should be considered a minimum. Sample FR14-01-31 was excluded based on a Grubbs' test for outliers (Grubbs, 1969).

The remaining four samples from the lateral yield ages ranging from 17,840 ± 420 to 16,200 ± 400 yr BP, with a mean of 17,100 ± 860 yr BP. Inboard of M0, we recognized a series of intermittent, low-relief moraines and planar surfaces with a pronounced ice-proximal scarp interpreted as kame terraces; we consider these to be recessional features not indicative of major glacier expansions. Their presence suggests ice retreat from M0 was incremental, but the lack of age control prohibits a quantitative interpretation of rate of retreat.

4.2. Moraine M1: 13520 ± 540 yr BP (n = 4, 1 outlier excluded)

The next prominent moraine upriver corresponds to M1, a sharp-crested frontal-lateral moraine (max. 50 m tall) ~4.3 km from the present ice margin. This moraine forms the most prominent moraine in the upper Río Fitz Roy valley. Several generations of outwash lie outboard of this landform, comprising the majority of the valley fill. The moraine is breached in several parts by streams and debris flows originating from the northern valley wall, but the lateral M1 moraine can be followed upriver beyond the current proglacial lake margin.

Five samples were used to constrain the age of this moraine; sample FR14-01-02 was excluded based on a Grubbs' test for outliers (Grubbs, 1969). This sample was taken from a location close to a gully that carried sediment from the slope above, which may have altered the original position of the boulder. The other four samples collected along the moraine front yield an average age of 13,520 ± 540 yr BP.

4.3. Moraine M2: 11,660 ± 260 to 9390 ± 180 yr BP (average 9730 ± 420 yr BP; n = 6)

M2 consists of a max. 30 m tall frontal-lateral moraine bisected by the Río Fitz Roy at about 3.2 km from the present ice margin. The northern lateral consists of a 10–20 m tall sharp-crested moraine cut in several parts by perennial streams originating from the northern valley wall. It grades into an elevated hummocky surface

Table 1
Analytical data for samples, sorted by moraine. An assumed sample density of 2.7 g/cm^3 is used in keeping with the felsic to intermediate lithologies sampled. Carrier concentrations used are 1048 ppm ([a]), 1043 ppm ([b]), and 1045 ppm ([c]). (*)AMS ratios presented as boron-corrected values measured against the 07KNSTD3110 standard material (^{10}Be/^{9}Be = 2.85 × 10^{-12}; Nishiizumi et al. 2007). Ratios are not corrected for background ^{10}Be in procedural blanks. (†) = ^{10}Be concentrations in this column are corrected for background ^{10}Be as recorded by the procedural blanks associated with each sample set, the concentrations of which ranged from 6.7545 × 10^{-17} to 7.6323 × 10^{-16}. (‡) = Moraine ages are reported as mean ages (excluding outliers; see text); reported error incorporates one standard deviation and the propagated 3% error of the production rate of Kaplan et al. (2011).

Moraine	Sample	CAMS	Lat.	Lon.	Elevation	Thickness	Shielding	Mass	Be carrier	^{10}Be/^{9}Be	^{10}Be	Age	1σ
		lab no.	°	°	m amsl	cm		g	g	(10^{-14})*	10^4 atoms/g†	yr BP	yr BP‡
M0	FR14-01-28	BE40834	−49.3274	−72.9433	666	2.5	0.993	10.8042	0.1822[a]	10.0665 ± 0.24422	11.845 ± 0.2876	16200	400
	FR14-01-29	BE40015	−49.3276	−72.9421	666	2.3	0.994	9.2087	0.1816[b]	9.6525 ± 0.22321	13.196 ± 0.3058	17840	420
	FR14-01-30	BE42008	−49.3277	−72.9416	659	2.8	0.994	10.0643	0.1816[c]	10.0434 ± 0.20771	12.581 ± 0.2608	17320	360
	FR14-01-31	*BE40016*	*−49.3281*	*−72.9407*	*667*	*2.2*	*0.994*	*10.8238*	*0.1819[b]*	*12.6727 ± 0.20360*	*14.783 ± 0.2381*	*19960*	*320*
	FR14-01-32	BE41998	−49.3281	−72.9405	668	2.6	0.994	10.0632	0.1820[c]	9.8830 ± 0.18340	12.476 ± 0.2318	17020	320
	Average											**17100**	**860**
M1	FR14-01-01	BE40253	−49.3268	−72.9644	640	2.7	0.983	30.1487	0.1822[b]	23.3169 ± 0.37580	9.803 ± 0.1581	13870	230
	FR14-01-02	*BE41991*	*−49.3258*	*−72.9668*	*631*	*2.7*	*0.981*	*10.0594*	*0.1826[c]*	*4.1679 ± 0.09756*	*5.276 ± 0.1240*	*7580*	*180*
	FR14-01-03	BE41992	−49.3276	−72.9626	623	2.3	0.982	10.6287	0.1819[c]	8.0449 ± 0.17528	9.608 ± 0.2096	13770	300
	FR14-01-04	BE40831	−49.3286	−72.961	625	2.1	0.988	25.0633	0.1825[a]	18.1621 ± 0.33641	9.243 ± 0.1713	13130	240
	FR14-01-05	BE40254	−49.3286	−72.961	621	1.7	0.987	27.3342	0.1817[b]	20.2526 ± 0.37771	9.362 ± 0.1747	13320	250
	Average											**13520**	**540**
M2	FR14-01-09	BE41993	−49.3244	−72.9792	630	2.5	0.973	10.0648	0.1824[c]	5.4675 ± 0.16690	6.912 ± 0.2113	9980	310
	FR14-01-10	*BE41994*	*−49.3255*	*−72.977*	*625*	*2.1*	*0.979*	*10.5112*	*0.1819[c]*	*6.4099 ± 0.12360*	*7.739 ± 0.1497*	*11110*	*215*
	FR14-01-13	BE40255	−49.3273	−72.9741	607	3.4	0.982	35.2886	0.1818[b]	18.6569 ± 0.39435	6.683 ± 0.1414	9820	210
	FR14-01-14	*BE41995*	*−49.3271*	*−72.9742*	*610*	*2.8*	*0.983*	*10.054*	*0.1721[c]*	*6.0254 ± 0.12235*	*7.195 ± 0.1465*	*10480*	*210*
	FR14-01-15	BE40256	−49.3276	−72.9741	605	1.6	0.982	35.0604	0.1813[b]	17.9895 ± 0.33616	6.467 ± 0.1210	9390	180
	FR14-01-16	*BE40832*	*−49.3288*	*−72.9738*	*606*	*2.0*	*0.986*	*25.07*	*0.1824[a]*	*15.8486 ± 0.35158*	*8.057 ± 0.1788*	*11660*	*260*
	Average											**9730**	**420**
M3	FRY16-02-08	BE42000	−49.3228	−72.9894	674	0.8	0.972	13.4369	0.1813[c]	5.3837 ± 0.12178	5.016 ± 0.1143	6910	130
	FRY16-02-09	BE42001	−49.3229	−72.9884	663	2.3	0.972	14.9972	0.1825[c]	5.8200 ± 0.11890	4.895 ± 0.1008	6710	130
	FRY16-02-10	BE42002	−49.3236	−72.9879	676	1.3	0.974	13.0344	0.1813[c]	5.1809 ± 0.11662	4.974 ± 0.1129	6900	130
	FR14-01-24	BE40833	−49.3264	−72.9851	654	1.5	0.982	25.0654	0.1828[a]	9.7240 ± 0.18719	4.948 ± 0.0954	6920	160
	FR14-01-25	BE40257	−49.3283	−72.9825	645	1.6	0.986	34.2906	0.1807[b]	13.0623 ± 0.24407	4.781 ± 0.0895	6890	140
	FR14-01-26	BE40258	−49.3294	−72.982	639	1.9	0.987	30.0048	0.1815[b]	11.6508 ± 0.21774	4.893 ± 0.0916	6860	160
	Average											**6860**	**220**
M4a	FR14-01-17	BE40828	−49.3308	−72.9834	669	2.2	0.988	50.0674	0.1820[a]	17.0830 ± 0.31598	4.340 ± 0.0803	5990	110
	FR14-01-18	BE41996	−49.3293	−72.9836	667	2.0	0.986	15.0561	0.1720[c]	5.3497 ± 0.11209	4.263 ± 0.0896	5900	120
	FR14-01-19	BE41997	−49.3293	−72.9836	667	1.8	0.986	13.9391	0.1729[c]	5.3292 ± 0.19257	4.611 ± 0.1668	6370	230
	Average											**6080**	**310**
M4b	FR14-01-20	BE42003	−49.329	−72.9837	665	2.3	0.982	5.0263	0.1819[c]	1.3499 ± 0.05426	3.258 ± 0.1358	4560	190
	FR14-01-21	BE40829	−49.3266	−72.9865	668	2.7	0.982	28.2396	0.1825[a]	7.0460 ± 0.14780	3.172 ± 0.0667	4450	90
	Average											**4500**	**160**
M7	FRY16-02-01	BE42009	−49.3298	−72.988	658	1.8	0.984	70.3865	0.1824[c]	2.1653 ± 0.13275	0.3781 ± 0.0233	560	40
	FRY16-02-03	BE42010	−49.3284	−72.9878	674	2.6	0.984	71.351	0.1820[c]	1.7775 ± 0.07427	0.3031 ± 0.0129	460	20
	FRY16-02-04	BE42011	−49.3273	−72.9884	675	1.5	0.984	73.9716	0.1816[c]	2.1852 ± 0.16986	0.3616 ± 0.0282	530	42
	Average											**520**	**60**

with no clear single ridge in the frontal section of the moraine.

Six samples from M2 yield ages from 11,700 ± 260 to 9390 ± 180 yr BP. Although these ages collectively do not overlap, and therefore do not provide a mean age (Fig. S2), the three youngest ages form a population with a mean age of 9730 ± 420 yr BP. We tentatively use this population in our discussion but emphasize that these ages solely record with confidence an early Holocene maximum of Glaciar Torre. Possible causes of this spread in ages include a period of glacier margin expansion during the latter interval of our age spread, long-term occupancy of the moraine by Glaciar Torre, or alternatively post-depositional collapse or reworking of the moraine front.

4.4. Moraine M3: 6860 ± 220 yr BP (n = 6)

Less than 700 m upstream, the M3 moraine complex consists of several tightly clustered lateral ridges that collectively rise over 50 m from the valley bottom 2.5 km from the ice margin, consisting of no fewer than three crests. Although these crests are distinct in the northern lateral section of the moraine, the frontal moraines have been mostly dissected by meltwater channels, forming a series of discontinuous ridges, hampering correlation of these frontal ridges with their lateral counterparts.

Three samples collected from boulders on the outermost lateral crest of M3 yield ages of 6920 ± 160, 6890 ± 140 and 6860 ± 160 yr BP. Three additional samples collected from the frontal M3 crest provided ages of 6910 ± 130, 6900 ± 130 and 6710 ± 130 yr BP. We treat samples taken from the frontal moraine fragments (n = 3) as equivalent to samples taken from the exterior lateral crest (n = 3); as they all overlap at 1-sigma, they are statistically indistinguishable and yield a uniform age of 6860 ± 220 yr BP for the entire moraine complex.

4.5. Moraine M4: 6080 ± 310 yr BP (n = 3) and 4510 ± 160 yr BP (n = 2)

M4 is a prominent (~60 m) moraine belt preserved on both sides of the river, 2.4 km from the ice margin. The moraine system partially overprints the M3 complex. The Río Fitz Roy runs parallel to the southern section of the moraine; evident slope retreat and subsequent erosion of the ridge crest led us to focus our sampling efforts only on the north side. The northern crest is continuous as a single mappable body but features a considerable vertical “step” between the higher frontal section and the lower lateral section, suggesting a geomorphic break.

The older frontal section yields ages of 6370 ± 230, 5990 ± 110

and 5900 ± 120 yr BP (M4a; mean age 6080 ± 310 yr BP), whereas the two samples from the lateral-lower section provide ages of 4560 ± 190 and 4,450 ± 90 yr BP (M4b; mean age 4510 ± 160 yr BP). Considered separately, two population clusters appear, the frontal at 6080 ± 310 yr BP, and the lateral at 4510 ± 160 yr BP, suggesting the present landform represents two distinct mid-Holocene glacier maxima. We therefore interpret M4 as a polygenetic landform, formed during two discrete mid-Holocene glacier advances at c. 6100 ka and c. 4500 ka.

4.6. Moraines M5 and M6: No absolute age control

M5 and M6 are represented by remnants of moraine ridges, interpreted by previous workers (Mercer, 1965; Masiokas et al., 2009) as evidence of two separate advances. We have no absolute age control for these moraines due to the poor preservation of these landforms and lack of suitable boulders for sampling. Based on their morphostratigraphic position, M5 and M6 must postdate the M4b advance at 4.5 ka and predate the later M7 advance.

4.7. Moraine M7: 520 ± 60 yr BP (n = 3)

Moraine M7 forms the innermost moraine crest bordering Laguna Torre, 2.1 km from the present ice margin. In the lateral sections the distinction between M6 and M7 is unclear. In parts M7 is recognizable as a trimline interior to the M6 crest, but in other parts the M7 lateral appears to merge or overprint the M6 lateral. M7 is only present north of the Río Fitz Roy. As a result, we did not sample from the M6 lateral, and focused our efforts on the unambiguous frontal crest of M7.

Three samples from boulders atop the sharp-crested frontal section of this moraine provide ages of 560 ± 40, 530 ± 40 and 460 ± 20 yr BP, with a mean age of 520 ± 60 yr BP. We attribute the relatively high chi-squared value of these ages to a) the high absolute precision of these dates, with analytical error on the order of tens of years; and b) the higher relative influence of pre-depositional ^{10}Be accumulated during supraglacial transport (inheritance) on younger age populations in alpine glaciers, a phenomenon discussed by Schaefer et al. (2009). Taken together, these ages indicate glacier advance between 400 and 600 years BP (15th-17th centuries CE). This age represents the most recent major moraine-building event by Glaciar Torre.

5. Discussion

Our results comprise the most comprehensive directly-dated chronology for fluctuations of a single Patagonian glacier spanning the last ~18,000 years. This chronology suggests that Glaciar Torre expanded coeval with a final phase of the LGM (M0: 17,100 ± 860 yr BP) and the Antarctic Cold Reversal (ACR) between 14,500 and 12,700 yr BP (M1: 13,520 ± 540 yr BP). Successively less-extensive expansions of Glaciar Torre reached maxima between 11,600 ± 260 and 9390 ± 180 yr BP (mean age 9730 ± 420 yr BP); and at 6860 ± 220, 6080 ± 310, 4510 ± 160, and 520 ± 60 yr BP; these maxima were separated in parts by millennial-scale periods when glacier advances were not preserved in the moraine record. While the LGM and ACR advances reflect well-documented events in Patagonia (García et al., 2012; Sagredo et al., 2018), the Holocene behavior of Glaciar Torre runs counter to the Hypsithermal/Neoglacial model proposed for the region (Porter, 2000) and demonstrates that previous studies considerably underestimated the ages of glacier advances in the area (Table 2).

5.1. Representativity of moraine ages

Analytical error of individual ages does not, in general, exceed 3% (Table S1). Holocene moraine age populations exhibit error on the order of hundreds of years, with reduced chi-squared values of less than 3 for all moraines save the youngest. For these youngest ages, increased analytical error (6–7%) and increased scatter ($\chi^2 = 6.3$; Supplementary Figs. S2 and S3) can be explained as a consequence of the very low concentrations of beryllium-10 in these samples and inheritance on very young landforms, respectively (Schaefer et al., 2009). While we recognize that moraine stabilization is not necessarily an instantaneous process, the minimal scatter of moraine ages therefore suggests that post-depositional reworking has not been an important factor on most of the dated moraines, giving us confidence that our record is an accurate record of glacier fluctuations at the centennial scale.

Single-glacier records suffer from the doubt that they may experience undue influence from microclimatic effects or even internal dynamics, complicating climatic interpretations of glacier advances. To test the representativity of our record, we compare our chronology to those of two outlet glaciers of the SPI, the Upsala glacier (Herminita and Pearson moraines) and the Frías glacier (Figs. 1a and 51°S). These constitute the most thorough records of directly-dated glacier fluctuations since late-glacial time in the region (Strelin et al., 2014; Kaplan et al., 2016). These records from Lago Argentino show glacier expansions during the ACR and at 6100 ± 390, 4450 ± 220, 2300-2000, 1400 ± 110, 600-500, 360 ± 30, and 240 ± 20 yr BP (Fig. 2b). Moreover, less well-dated positions are at ~5500 and 2300-2000 yr BP (Strelin et al., 2014).

Our records overlap during the ACR (Kaplan et al., 2011) and at 6100, 4500, and 600-500 yr BP. We argue the pre-6000 yr BP events not preserved at Lago Argentino reflect climatic events within a generalized warm period on a scale too brief for the much larger SPI to respond and leave a preserved moraine record (Jóhannesson et al., 1989). Within dating uncertainties, early Holocene glaciers at Lago Argentino remained close to the 20th century limits during this time period (Strelin et al., 2014), suggesting any activity would

Table 2
Moraine ages from this study from Table 1 compared with previous age constraints.

Landform	Age (this study)	Age (previously reported)	Type of measurement	Reference
	yr BP	yr BP (2016)		
M0	17,100 ± 860	–	–	–
M1	13,520 ± 540	>535	Lichenometry	Garibotti and Villalba (2009)
M2	9730 ± 420	>273	Lichenometry	Garibotti and Villalba (2009)
M3	6,860 ± 220	>392	Tree ring surface exposure	Masiokas et al. (2009)
		>800 ± 85 (^{14}C yr BP)	Age of inboard basal peat	Mercer (1965)
M4a	6,080 ± 310	–	–	–
M4b	4,500 ± 160	>360	Tree ring surface exposure	Masiokas et al. (2009)
		~320	Tree ring surface exposure	Mercer (1965)
M7	520 ± 60	>175	Lichenometry	Garibotti and Villalba (2009)

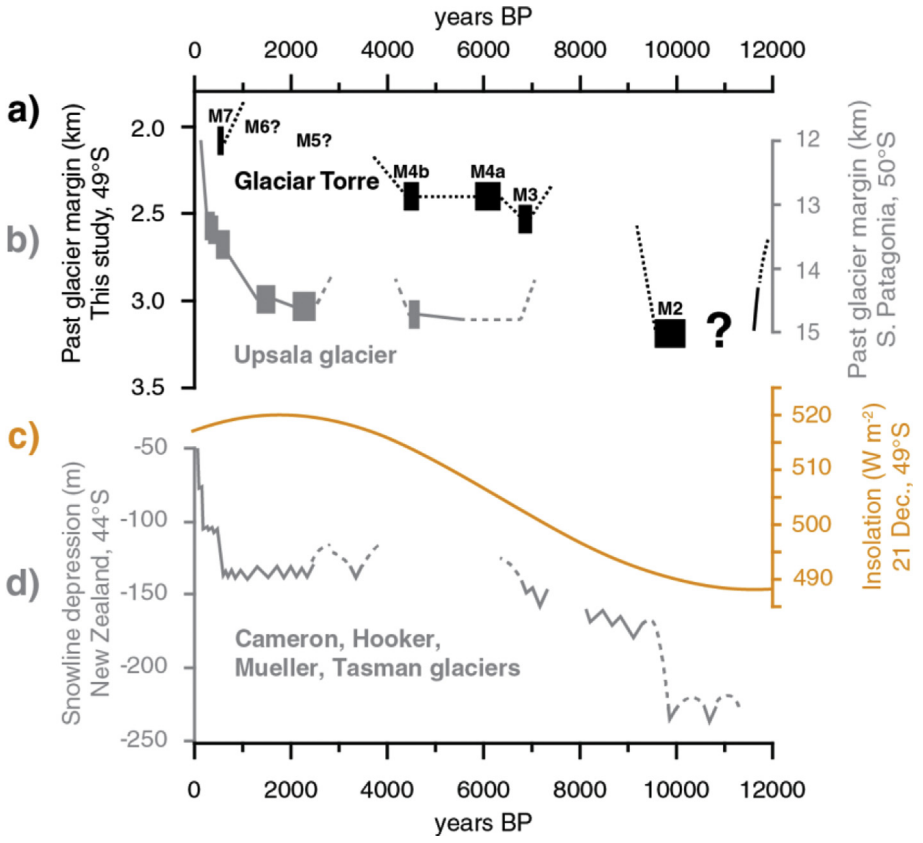

Fig. 2. a) Time-distance diagram of Glaciar Torre moraines. Boxes are mean moraine ages with ±1-sigma uncertainty. Lines indicate inferred glacier behavior; question marks indicate inferred times at which a moraine is found a certain distance from the ice margin. b) Time-distance diagram of Upsala glacier (Kaplan et al., 2016), based on chronologies from Peninsula Herminita and Lago Pearson. c) Summer insolation intensity at 49°S (Laskar et al., 2004). d) Composite snowline depression from the South Island of New Zealand (Putnam et al., 2012). Solid lines correspond to dated glacier advances; dashed lines correspond to inferred glacier retreat.

have been erased by subsequent extensive mid-Holocene glaciers. Glacier advances between 2300-2000 and 1450-1100 yr BP, recorded at Lago Argentino, correspond morphostratigraphically with our M5 and M6 moraines, which were unsuitable for dating. Given the observed parallels between our glacier chronologies, we suggest both glacier systems responded to similar external forcings, rather than internal variability. We merge both chronologies using these advances as tie points to yield a composite Holocene glacier chronology for southern Patagonia. Together, these observations reveal a regional pattern of steadily-declining glacier expansions throughout the Holocene (Fig. 2).

5.2. Insolation as "modulator" of Holocene glaciers

Our composite glacier chronology from southern Patagonia (Fig. 2a and b) mirrors the pattern of progressively less-extensive Holocene glacier advances in New Zealand (Fig. 2d), although the timing of discrete advances differs. We first address the zonally-uniform trend of declining Holocene glacier extent in the southern mid-latitudes, a pattern different to that of the northern mid-latitudes. Summer insolation intensity increases (decreases) from the early to the late Holocene in the Southern (Northern) Hemisphere (Laskar et al., 2004) (Fig. 2c), suggesting that this factor played a key role in modulating global glacier extent during this period. As local summer insolation intensity relates inversely to summer duration (Huybers and Denton, 2008), the former likely is more influential in constraining mid-latitude glacier extent during the latest interglacial.

While parallel trends of insolation and glacier extent could be due to a direct, glacier-specific effect of secular insolation change on glacier mass balance, indirect effects cannot be ruled out. Mid-Holocene glacier reconstructions from Patagonia and New Zealand suggest glaciers in both zones responded to depressed temperatures forced by lower summer insolation (Bravo et al., 2015; Rojas and Moreno, 2011). Modelled cool mid-Holocene conditions in both Patagonia (Wagner et al., 2007) and New Zealand (Ackerley et al., 2013) have been attributed to insolation-modulated changes on the zonal westerlies, meridional temperature gradients, and local land surface temperature. An insolation-modulated migration of the Intertropical Convergence Zone has also been proposed to explain the trend of declining Southern Hemisphere glacier extent during the Holocene (Putnam et al., 2012).

5.3. The SAM as "pacemaker" of Patagonian climate

Progressive change in summer insolation intensity cannot by itself produce the observed repeated glacier advances in Patagonia—a forcing that provides periodic "kicks" to the climate system is necessary. Although the overlap between our record and those at Lago Argentino suggest regionally impactful changes in climate occurred periodically throughout the Holocene, it has been proposed that such variations could be due to effectively random climate excursions on a scale not exceeding that observed on the decadal timeframe (Roe and O'Neal, 2009). As a test of whether our observed glacier variability is observed in other terrestrial paleoclimate proxies, we refer to a recent palynological study of lake sediments from Lago Cipreses, located ~220 km south from Glaciar Torre (Fig. 1a). Here, Moreno et al. (2018) identified warm/dry

secular events with an average duration of 200 ± 60 years since 11,000 yr BP, which alternated with cold/wet phases lasting on average 500 ± 200 years. These phases are tentatively connected to long-term trends in the SAM, the variability of which would also have direct effects on Patagonian glaciers. Modern variability of the SAM drives anomalies in temperature and the SWW during the summer months throughout Patagonia, with positive (negative) SAM indices correlated to higher (lower) summer temperatures (Garreaud et al., 2009) and a corresponding redistribution of precipitation across the orographic divide (Garreaud et al., 2013).

Comparison of our ensemble chronology with the Lago Cipreses non-arboreal pollen (NAP) record (Fig. 3), a proxy for climate-induced intervals of forest canopy opening and closure, suggests that Patagonian glaciers reached their maxima during centennial- to millennial-scale SAM-negative-like phases. Conversely, prolonged SAM-positive-like phases—the Extended Warm Dry Anomaly (EWDA, 9500-7500 yr BP) and the Late Holocene Warm Dry Period (LHWDP, 4100-2800 yr BP)—correspond to periods when Patagonian glaciers were less-extensive (Fig. 3). Other dated moraines from the Colonia valley (Nimick et al., 2016) and Río Tranquilo (Sagredo et al., 2016) (Figs. 1a and 3d), as well as the few closely-bracketed ages of glacial sediment from the historical literature (Fig. 3e; Mercer, 1965; Röthlisberger, 1986; Harrison et al., 2012; Strelin et al., 2014), corroborate this pattern.

The correspondence between our composite glacier chronology and paleoecological changes at Lago Cipreses leads us to suggest that Patagonian glacier advances were paced by centennial-scale climate variability—resembling that of the modern SAM—that resulted in warm or cool periods throughout the Holocene. In this scenario, the hypothesized paleo-SAM would have modulated glacier mass balance via its effect on summer temperature, reflecting the modern climatology. Other potential drivers of Patagonian climate include the modes of climate variability in the south Pacific, the El Niño- Southern Oscillation phenomenon (ENSO) and the Interdecadal Pacific Oscillation/Pacific Decadal Oscillation (IPO/PDO). ENSO and the IPO/PDO, however, have not been shown to significantly affect modern interannual variability of precipitation or temperature in central and southern Patagonia (Garreaud et al., 2009), although a centennial-scale relationship between ENSO and SAM may exist over the Holocene (Moy et al., 2002; Yuan et al., 2018; Moreno et al., 2018). This differs from the New Zealand case, where ENSO and the IPO/PDO currently exert a strong influence in the southwestern Pacific climate (Salinger and Mullan, 1999). Meridional shifts of warm anomalies related to the central and eastern modes of ENSO (Carré et al., 2014) may account for differences in the timing of Holocene glacier advances between Patagonia and New Zealand (Fig. 2).

Our results suggest that Patagonian glaciers responded to two mechanisms during the Holocene: a global, insolation-driven "modulator" governing the magnitude of a glacier response; and a regional, SAM-like "pacemaker" that determines the timing of glacier change. Within this context, summer insolation intensity plays an important role in regulating ice extent in both hemispheres' midlatitudes under interglacial conditions. Future work is

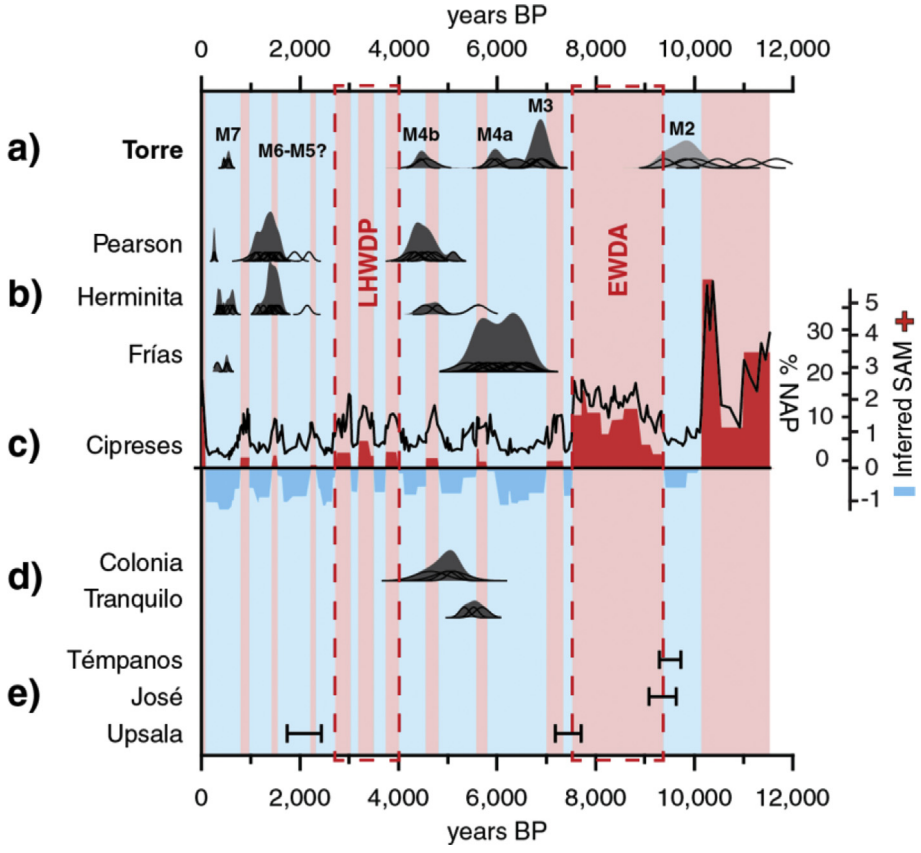

Fig. 3. Southern Patagonian paleoglacier records for a) Glaciar Torre and b) Lago Argentino (Strelin et al., 2014; Kaplan et al., 2016). ^{10}Be ages are presented as normalized standard probability distributions (black curves); cumulative weighted average moraine ages are represented by shaded curves. Shading represents inferred SAM (red = positive; blue = negative) from c) the Lago Cipreses (Moreno et al., 2018) non-arboreal pollen (NAP) record (black line) and regime shift detection z-scores (colored polygons). LHWDP = Late Holocene Warm Dry Period; EWDA = Early Warm Dry Anomaly. d) Other published ^{10}Be moraine ages in southern Patagonia: Colonia (Nimick et al., 2016) and Río Tranquilo (Sagredo et al., 2016). e) All close bracketing ages of glacial deposits from Patagonia: Témpanos (OSL) (Harrison et al., 2012), José (^{14}C) (Röthlisberger, 1986), and Upsala (^{14}C) (Mercer, 1965; Strelin et al., 2014). (For interpretation of the references to color in this figure legend, the reader is referred to the Web version of this article.)

needed to determine the specific avenue through which insolation could have affected glaciers.

The modern trend towards high-index SAM conditions in austral summer has been explained as a consequence of greenhouse gas forcing and stratospheric ozone depletion; future implementation of the Montreal Protocol is postulated to inhibit this positive trend (Thompson et al., 2011). We note, however, that our record suggests the observed trend may be superimposed upon a larger shift in baseline climate (Zhang et al., 2014). The present effects of positive SAM on the southern midlatitudes—the southward shift and intensification of the westerlies, summer warming, and precipitation redistribution (Gillett et al., 2006)—may therefore represent the new normal climate that may persist for hundreds of years, independent of future changes in anthropogenic forcings.

Acknowledgements

This project was supported by the Núcleo Milenio Paleoclima of the Iniciativa Científica Milenio of the Ministerio de Economía, Fomento y Turismo (Chile), FONDECYT 1160488, FONDECYT 1171773, FONDECYT 1180717, FONDAP-CONICYT 15110009, NSF-EAR 09-02363, and NSF-EAR 18–04816. S.A.R. is a recipient of a CONICYT-PCHA Beca de Doctorado Nacional (2015). We thank the Administración de Parques Nacionales and Parque Nacional Los Glaciares (Argentina) for their support. We additionally thank J. Hanley and J. Frisch for laboratory support; and P. Talbot, M. Calabrese, D. Tetzner, C. Sullivan, and G. Sullivan for scientific and logistical support in the field. This is LDEO contribution # 8326.

Appendix A. Supplementary data

Supplementary data to this article can be found online at https://doi.org/10.1016/j.quascirev.2019.05.029.

References

Abram, N.J., Mulvaney, R., Vimeux, F., Phipps, S.J., Turner, J., England, M.H., 2014. Evolution of the southern annular mode during the past millennium. Nat. Clim. Change 4, 564.

Ackerley, D., Lorrey, A., Renwick, J., Phipps, S.J., Wagner, S., Fowler, A., 2013. High-resolution modelling of mid-Holocene New Zealand climate at 6000 yr BP. Holocene 23, 1272–1285. https://doi.org/10.1177/0959683613484612.

Aniya, M., 2013. Holocene glaciations of Hielo Patagónico (Patagonia Icefield), south America: a brief review. Geochem. J. https://doi.org/10.2343/geochemj.1.0171.

Aniya, M., Sato, H., 1995. Holocene glacial chronology of Upsala glacier at Peninsula Herminita, southern Patagonia Icefield. Bull. Glacier Res. 13, 83–96.

Auer, V., 1956. The Pleistocene of Fuego-Patagonia. Part I: the Ice and Interglacial Ages, Series AII. Annales Academia Scientarium Fennicae, Helsinki.

Balco, G., Stone, J.O., Lifton, N.A., Dunai, T.J., 2008. A complete and easily accessible means of calculating surface exposure ages or erosion rates from 10Be and 26Al measurements. Quat. Geochronol. 3, 174–195. https://doi.org/10.1016/J.QUAGEO.2007.12.001.

Bravo, C., Rojas, M., Anderson, B.M., Mackintosh, A.N., Sagredo, E., Moreno, P.I., 2015. Modelled glacier equilibrium line altitudes during the mid-Holocene in the southern mid-latitudes. Clim. Past 11, 1575–1586. https://doi.org/10.5194/cp-11-1575-2015.

Carlson, A.E., Winsor, K., Ullman, D.J., Brook, E.J., Rood, D.H., Axford, Y., LeGrande, A.N., Anslow, F.S., Sinclair, G., 2014. Earliest Holocene south Greenland ice sheet retreat within its late Holocene extent. Geophys. Res. Lett. 41, 5514–5521. https://doi.org/10.1002/2014GL060800.

Carrasco, J.F., Casassa, G., Rivera, A., 2002. Meteorological and Climatological Aspects of the Southern Patagonia Icefield. In: Casassa, G., Sepúlveda, F.V., Sinclair, R.M. (Eds.), The Patagonian Icefields: A Unique Natural Laboratory for Environmental and Climate Change Studies. Springer, Boston, MA, pp. 29–41. https://doi.org/10.1007/978-1-4615-0645-4_4.

Carré, M., Sachs, J.P., Purca, S., Schauer, A.J., Braconnot, P., Falcón, R.A., Julien, M., Lavallée, D., 2014. Holocene history of ENSO variance and asymmetry in the eastern tropical Pacific. Science (80-.) 345, 1045 LP – 1048.

Clapperton, C.M., Sugden, D.E., 1988. Holocene glacier fluctuations in South America and Antarctica. Quat. Sci. Rev. 7, 185–198. https://doi.org/10.1016/0277-3791(88)90005-4.

Denton, G.H., Karlén, W., 1973. Holocene climatic variations-Their pattern and possible cause. Quat. Res. 3, 155–205. https://doi.org/10.1016/0033-5894(73)90040-9.

García, J.L., Kaplan, M.R., Hall, B.L., Schaefer, J.M., Vega, R.M., Schwartz, R., Finkel, R., 2012. Glacier expansion in southern Patagonia throughout the Antarctic cold reversal. Geology 40, 859–862.

Garibotti, I.A., Villalba, R., 2009. Lichenometric dating using Rhizocarpon subgenus Rhizocarpon in the Patagonian Andes, Argentina. Quat. Res. 71, 271–283. https://doi.org/10.1016/J.YQRES.2009.01.012.

Garreaud, R.D., Vuille, M., Compagnucci, R., Marengo, J., 2009. Present-day south American climate. Palaeogeogr. Palaeoclimatol. Palaeoecol. 281, 180–195. https://doi.org/10.1016/j.palaeo.2007.10.032.

Garreaud, R., Lopez, P., Minvielle, M., Rojas, M., 2013. Large-scale control on the Patagonian climate. J. Clim. 26, 215–230. https://doi.org/10.1175/JCLI-D-12-00001.1.

Gillett, N.P., Kell, T.D., Jones, P.D., 2006. Regional climate impacts of the southern annular mode. Geophys. Res. Lett. 33. https://doi.org/10.1029/2006GL027721.

Glasser, N.F., Harrison, S., Winchester, V., Aniya, M., 2004. Late Pleistocene and holocene palaeoclimate and glacier fluctuations in Patagonia. Glob. Planet. Chang. 43, 79–101. https://doi.org/10.1016/J.GLOPLACHA.2004.03.002.

Grubbs, F.E., 1969. Procedures for detecting outlying observations in samples. Technometrics 11, 1–21. https://doi.org/10.1080/00401706.1969.10490657.

Harrison, S., Glasser, N.F., Duller, G.A.T., Jansson, K.N., 2012. Early and mid-holocene age for the tempanos moraines, Laguna san Rafael, Patagonian Chile. Quat. Sci. Rev. 31, 82–92. https://doi.org/10.1016/J.QUASCIREV.2011.10.015.

Heim, A., 1951. Informe sobre un estudio glaciológico en el Parque Nacional Los Glaciares. Anales de Parques Nacionales, Buenos Aires.

Hogg, A.G., Hua, Q., Blackwell, P.G., Niu, M., Buck, C.E., Guilderson, T.P., Heaton, T.J., Palmer, J.G., Reimer, P.J., Reimer, R.W., Turney, C.S.M., Zimmerman, S.R.H., 2013. SHCal13 southern hemisphere calibration, 0–50,000 Years cal BP. Radiocarbon 55, 1889–1903. https://doi.org/10.2458/azu_js_rc.55.16783.

Huybers, P., Denton, G., 2008. Antarctic temperature at orbital timescales controlled by local summer duration. Nat. Geosci. 1, 787.

Ivy-Ochs, S., Kerschner, H., Maisch, M., Christl, M., Kubik, P.W., Schlüchter, C., 2009. Latest Pleistocene and Holocene glacier variations in the European Alps. Quat. Sci. Rev. 28, 2137–2149. https://doi.org/10.1016/j.quascirev.2009.03.009.

Jóhannesson, T., Raymond, C.F., Waddington, E.D., 1989. A Simple Method for Determining the Response Time of Glaciers. Springer, Dordrecht, pp. 343–352. https://doi.org/10.1007/978-94-015-7823-3_22.

Jones, J.M., Gille, S.T., Goosse, H., Abram, N.J., Canziani, P.O., Charman, D.J., Clem, K.R., Crosta, X., de Lavergne, C., Eisenman, I., England, M.H., Fogt, R.L., Frankcombe, L.M., Marshall, G.J., Masson-Delmotte, V., Morrison, A.K., Orsi, A.J., Raphael, M.N., Renwick, J.A., Schneider, D.P., Simpkins, G.R., Steig, E.J., Stenni, B., Swingedouw, D., Vance, T.R., 2016. Assessing recent trends in high-latitude Southern Hemisphere surface climate. Nat. Clim. Change 6, 917.

Kaplan, M.R., Strelin, J.A., Schaefer, J.M., Denton, G.H., Finkel, R.C., Schwartz, R., Putnam, A.E., Vandergoes, M.J., Goehring, B.M., Travis, S.G., 2011. In-situ cosmogenic 10Be production rate at Lago Argentino, Patagonia: implications for late-glacial climate chronology. Earth Planet. Sci. Lett. 309, 21–32. https://doi.org/10.1016/J.EPSL.2011.06.018.

Kaplan, M.R., Schaefer, J.M., Denton, G.H., Doughty, A.M., Barrell, D.J.A., Chinn, T.J.H., Putnam, A.E., Andersen, B.G., Mackintosh, A., Finkel, R.C., Schwartz, R., Anderson, B., 2013. The anatomy of long-term warming since 15 ka in New Zealand based on net glacier snowline rise. Geology 41, 887–890.

Kaplan, M.R., Schaefer, J.M., Strelin, J.A., Denton, G.H., Anderson, R.F., Vandergoes, M.J., Finkel, R.C., Schwartz, R., Travis, S.G., Garcia, J.L., Martini, M.A., Nielsen, S.H.H., 2016. Patagonian and southern South Atlantic view of holocene climate. Quat. Sci. Rev. 141, 112–125. https://doi.org/10.1016/j.quascirev.2016.03.014.

Kaufman, D., Ager, T., Anderson, N., Anderson, P., Andrews, J., Bartlein, P., Brubaker, L., Coats, L., Cwynar, L., Duvall, M., Dyke, A., Edwards, M., Eisner, W., Gajewski, K., Geirsdóttir, A., Hu, F., Jennings, A., Kaplan, M., Kerwin, M., Lozhkin, A., MacDonald, G., Miller, G., Mock, C., Oswald, W., Otto-Bliesner, B., Porinchu, D., Rühland, K., Smol, J., Steig, E., Wolfe, B., 2004. Holocene thermal maximum in the western Arctic (0–180°W). Quat. Sci. Rev. 23, 529–560. https://doi.org/10.1016/J.QUASCIREV.2003.09.007.

Laskar, J., Robutel, P., Joutel, F., Gastineau, M., Correia, A.C.M., Levrard, B., 2004. A long-term numerical solution for the insolation quantities of the Earth. A&A 428, 261–285.

Lawrence, D.B., Lawrence, E.G., 1959. Recent Glacier Variations in Southern South America. American Geographical Society Technical Report.

Lifton, N., Smart, D.F., Shea, M.A., 2008. Scaling time-integrated in situ cosmogenic nuclide production rates using a continuous geomagnetic model. Earth Planet. Sci. Lett. 268, 190–201. https://doi.org/10.1016/J.EPSL.2008.01.021.

Lliboutry, L., 1953. Snow and ice in the Monte Fitz Roy region (Patagonia). J. Glaciol. 2, 255–261. https://doi.org/10.3189/S0022143000025430.

Mackintosh, A.N., Anderson, B.M., Pierrehumbert, R.T., 2017. Reconstructing climate from glaciers. Annu. Rev. Earth Planet Sci. 45, 649–680. https://doi.org/10.1146/annurev-earth-063016-020643.

Masiokas, M.H., Luckman, B.H., Delgado, S., Skvarca, P., Ripalta, A., 2009. Little Ice Age fluctuations of small glaciers in the Monte Fitz Roy and Lago del Desierto areas, south Patagonian Andes, Argentina. Palaeogeogr. Palaeoclimatol. Palaeoecol. 281, 351–362. https://doi.org/10.1016/J.PALAEO.2007.10.031.

Mercer, J.H., 1965. Glacier variations in southern Patagonia. Geogr. Rev. 55, 390–413. https://doi.org/10.2307/213136.

Mercer, J.H., 1976. Glacial history of southernmost South America. Quat. Res. 6,

125–166. https://doi.org/10.1016/0033-5894(76)90047-8.
Mercer, J.H., 1982. Holocene Glacier Variations in Southern South America (Striae).
Miller, A., 1976. The climate of Chile. In: Schwerdtfeger, W. (Ed.), World Survey of Climatology. Elsevier, Amsterdam, pp. 113–130.
Moreno, P.I., Vilanova, I., Villa-Martínez, R., Dunbar, R.B., Mucciarone, D.A., Kaplan, M.R., Garreaud, R.D., Rojas, M., Moy, C.M., De Pol-Holz, R., Lambert, F., 2018. Onset and Evolution of southern annular mode-like changes at centennial timescale. Sci. Rep. 8, 3458. https://doi.org/10.1038/s41598-018-21836-6.
Moy, C.M., Seltzer, G.O., Rodbell, D.T., Anderson, D.M., 2002. Variability of El Niño/southern oscillation activity at millennial timescales during the holocene epoch. Nature 420, 162.
Nesje, A., 2009. Latest Pleistocene and holocene alpine glacier fluctuations in Scandinavia. Quat. Sci. Rev. 28, 2119–2136. https://doi.org/10.1016/j.quascirev.2008.12.016.
Nimick, D.A., McGrath, D., Mahan, S.A., Friesen, B.A., Leidich, J., 2016. Latest Pleistocene and holocene glacial events in the Colonia Valley, northern Patagonia Icefield, southern Chile. J. Quat. Sci. 31, 551–564. https://doi.org/10.1002/jqs.2847.
Olson, D.M., Dinerstein, E., Wikramanayake, E.D., Burgess, N.D., Powell, G.V.N., Underwood, E.C., D'amico, J.A., Itoua, I., Strand, H.E., Morrison, J.C., Loucks, C.J., Allnutt, T.F., Ricketts, T.H., Kura, Y., Lamoreux, J.F., Wettengel, W.W., Hedao, P., Kassem, K.R., 2001. Terrestrial Ecoregions of the World: a New Map of Life on EarthA new global map of terrestrial ecoregions provides an innovative tool for conserving biodiversity. Bioscience 51, 933–938. https://doi.org/10.1641/0006-3568(2001)051[0933:teotwa]2.0.co;2.
Porter, S.C., Denton, G.H., 1967. Chronology of neoglaciation in the north American Cordillera. Am. J. Sci. 265, 177–210. https://doi.org/10.2475/ajs.265.3.177.
Porter, S.C., 2000. Onset of neoglaciation in the southern hemisphere. J. Quat. Sci. 15, 395–408. https://doi.org/10.1002/1099-1417(200005)15:4%3c395::AID-JQS535%3e3.0.CO;2-H.
Putnam, A.E., Schaefer, J.M., Denton, G.H., Barrell, D.J.A., Finkel, R.C., Andersen, B.G., Schwartz, R., Chinn, T.J.H., Doughty, A.M., 2012. Regional climate control of glaciers in New Zealand and Europe during the pre-industrial Holocene. Nat. Geosci. 5, 627.
Rasmussen, L.A., Conway, H., Raymond, C.F., 2007. Influence of upper air conditions on the Patagonia icefields. Glob. Planet. Chang. 59, 203–216. https://doi.org/10.1016/J.GLOPLACHA.2006.11.025.
Rignot, E., Rivera, A., Casassa, G., 2003. Contribution of the Patagonia icefields of south America to Sea level rise. Science (80-.) 302, 434 LP – 437. https://doi.org/10.1126/science.1087393.
Rivera, A., Casassa, G., 2004. Ice Elevation, Areal, and Frontal Changes of Glaciers from National Park Torres del Paine, Southern Patagonia Icefield. Arctic. Antarct. Alp. Res. 36, 379–389. https://doi.org/10.1657/1523-0430(2004)036[0379:IEAAFC]2.0.CO;2.
Roe, G.H., O'Neal, M.A., 2009. The response of glaciers to intrinsic climate variability: observations and models of late-Holocene variations in the Pacific Northwest. J. Glaciol. 55, 839–854. https://doi.org/10.3189/002214309790152438.
Rojas, M., Moreno, P.I., 2011. Atmospheric circulation changes and neoglacial conditions in the Southern Hemisphere mid-latitudes: insights from PMIP2 simulations at 6 kyr. Clim. Dyn. 37, 357–375. https://doi.org/10.1007/s00382-010-0866-3.
Röthlisberger, F., 1986. 1000 Jahre Gletschergeschichte der Erde. Verlag Sauerlander, Salzburg.
Sagredo, E.A., Lowell, T.V., Kelly, M.A., Rupper, S., Aravena, J.C., Ward, D.J., Malone, A.G.O., 2016. Equilibrium line altitudes along the Andes during the Last millennium: Paleoclimatic implications. Holocene 27, 1019–1033. https://doi.org/10.1177/0959683616678458.
Sagredo, E.A., Kaplan, M.R., Araya, P.S., Lowell, T.V., Aravena, J.C., Moreno, P.I., Kelly, M.A., Schaefer, J.M., 2018. Trans-pacific glacial response to the Antarctic Cold Reversal in the southern mid-latitudes. Quat. Sci. Rev. 188, 160–166. https://doi.org/10.1016/J.QUASCIREV.2018.01.011.
Sagredo, E.A., Rupper, S., Lowell, T.V., 2014. Sensitivities of the equilibrium line altitude to temperature and precipitation changes along the Andes. Quat. Res. 81, 355–366. https://doi.org/10.1016/j.yqres.2014.01.008.
Salinger, M.J., Mullan, A.B., 1999. New Zealand climate: temperature and precipitation variations and their links with atmospheric circulation 1930–1994. Int. J. Climatol. 19, 1049–1071. https://doi.org/10.1002/(SICI)1097-0088(199908)19:10%3c1049::AID-JOC417%3e3.0.CO;2-Z.
Schaefer, J.M., Denton, G.H., Kaplan, M., Putnam, A., Finkel, R.C., Barrell, D.J.A., Andersen, B.G., Schwartz, R., Mackintosh, A., Chinn, T., Schlüchter, C., 2009. High-frequency holocene glacier fluctuations in New Zealand differ from the northern signature. Science 84.) 324, 622–625. https://doi.org/10.1126/science.1169312.
Schaefer, M., Machguth, H., Falvey, M., Casassa, G., Rignot, E., 2015. Quantifying mass balance processes on the southern Patagonia Icefield. Cryosph 9, 25–35. https://doi.org/10.5194/tc-9-25-2015.
Schimmelpfennig, I., Schaefer, J.M., Akçar, N., Ivy-Ochs, S., Finkel, R.C., Schlüchter, C., 2012. Holocene glacier culminations in the Western Alps and their hemispheric relevance. Geology 40, 891–894.
Solomina, O.N., Bradley, R.S., Hodgson, D.A., Ivy-Ochs, S., Jomelli, V., Mackintosh, A.N., Nesje, A., Owen, L.A., Wanner, H., Wiles, G.C., Young, N.E., 2015. Holocene glacier fluctuations. Quat. Sci. Rev. https://doi.org/10.1016/j.quascirev.2014.11.018.
Strelin, J.A., Denton, G.H., Vandergoes, M.J., Ninnemann, U.S., Putnam, A.E., 2011. Radiocarbon chronology of the late-glacial Puerto Bandera moraines, southern Patagonian Icefield, Argentina. Quat. Sci. Rev. 30, 2551–2569. https://doi.org/10.1016/J.QUASCIREV.2011.05.004.
Strelin, J.A., Kaplan, M.R., Vandergoes, M.J., Denton, G.H., Schaefer, J.M., 2014. Holocene glacier history of the Lago Argentino basin, southern Patagonian Icefield. Quat. Sci. Rev. 101, 124–145. https://doi.org/10.1016/j.quascirev.2014.06.026.
Stuiver, M., Reimer, P.J., 2018. CALIB.
Thompson, D.W.J., Solomon, S., Kushner, P.J., England, M.H., Grise, K.M., Karoly, D.J., 2011. Signatures of the Antarctic ozone hole in Southern Hemisphere surface climate change. Nat. Geosci. 4, 741.
Villalba, R., Lara, A., Boninsegna, J.A., Masiokas, M., Delgado, S., Aravena, J.C., Roig, F.A., Schmelter, A., Wolodarsky, A., Ripalta, A., 2003. Large-scale temperature changes across the southern Andes: 20th-century variations in the context of the past 400 years. Clim. Change 59, 177–232. https://doi.org/10.1023/A:1024452701153.
Villalba, R., Lara, A., Masiokas, M.H., Urrutia, R., Luckman, B.H., Marshall, G.J., Mundo, I.A., Christie, D.A., Cook, E.R., Neukom, R., Allen, K., Fenwick, P., Boninsegna, J.A., Srur, A.M., Morales, M.S., Araneo, D., Palmer, J.G., Cuq, E., Aravena, J.C., Holz, A., LeQuesne, C., 2012. Unusual southern hemisphere tree growth patterns induced by changes in the southern annular mode. Nat. Geosci. 5, 793.
Wagner, S., Widmann, M., Jones, J., Haberzettl, T., Lücke, A., Mayr, C., Ohlendorf, C., Schäbitz, F., Zolitschka, B., 2007. Transient simulations, empirical reconstructions and forcing mechanisms for the Mid-holocene hydrological climate in southern Patagonia. Clim. Dyn. 29, 333–355. https://doi.org/10.1007/s00382-007-0229-x.
Yuan, X., Kaplan, M.R., Cane, M.A., 2018. The interconnected global climate system-a review of tropical-polar teleconnections. J. Clim. 31, 5765–5792. https://doi.org/10.1175/JCLI-D-16-0637.1.
Zhang, Z., Gong, D., Kim, S., Mao, R., Yang, J., 2014. Is the Antarctic oscillation trend during the recent decades unusual? Antarct. Sci. 26, 445–451. https://doi.org/10.1017/S0954102013000734.

Supplementary Information for

Holocene glacier fluctuations in Patagonia are modulated by summer insolation intensity and paced by Southern Annular Mode-like variability

Scott A. Reynhout[1,2], Esteban A. Sagredo*[2,3], Michael R. Kaplan[4,5], Juan Carlos Aravena[2,5], Mateo A. Martini[6,7], Patricio I. Moreno[2,8], Maisa Rojas[2,9], Roseanne Schwartz[4], and Joerg M. Schaefer[4,10]

[1]*Departamento de Geología, Facultad de Ciencias Físicas y Matemáticas, Universidad de Chile, Plaza Ercilla 803, 8370450 Santiago, Chile*

[2]*Núcleo Milenio Paleoclima, Universidad de Chile, Las Palmeras 3425, Ñuñoa, Chile*

[3]*Instituto de Geografía, Pontificia Universidad Católica de Chile, Avenida Vicuña Mackenna 4860, 7820436 Macul, Chile*

[4]*Lamont-Doherty Earth Observatory, P.O. Box 1000, 61 Route 9W, Palisades, NY 10964-100, United States of America*

[5]*Centro de Investigación Gaia Antártica, Universidad de Magallanes, Avenida Bulnes 01855 62000009, Punta Arenas, Chile*

[6]*Centro de Investigaciones en Ciencias de la Tierra (CONICET-UNC), Vélez Sársfeld 1611, X5016GCA, Córdoba, Argentina*

[7]*Facultad de Ciencias Exactas, Físicas y Naturales (Universidad Nacional de Córdoba), Vélez Sársfled 1611, X5016GCA, Córdoba, Argentina*

[8]*Departamento de Ciencias Ecológicas, Facultad de Ciencias, Universidad de Chile, Las Palmeras 3425, Ñuñoa, Chile*

[9]*Departamento de Geofísica, Facultad de Ciencias Físicas y Matemáticas, Universidad de Chile, Avenida Blanco Encalada 2002, Santiago, Chile*

[10]*Department of Earth and Environmental Sciences of Columbia University, New York, NY, 10027, USA*

This file includes:

Comparison of results with historical records

Of the seven moraines dated in our study, six have previously-reported age constraints. The ages we obtained for moraines M1-M7 differ significantly from the radiocarbon, lichenometric, and dendrochronologic age constraints obtained by previous workers (Mercer, 1965; Garibotti and Villalba, 2009; Masiokas et al., 2009) (Table S2). In the case of M3 and M4 this was not unexpected, as the ~400-year-old ages of *Nothofagus betuloides* used by Masiokas et al. (2009) approached the maximum living age of these trees in such climate conditions. However, it is noteworthy that our c. 1500 CE age for the treeless M7 moraine predates the oldest trees in the study area. As growth has not begun on this moraine, which is older than the maximum age of *Nothofagus betuloides*, this suggests that previously-suggested ecesis intervals for this region must be applied with caution.

Mercer (1965) obtained a minimum-limiting age for the M3 complex of 800 ± 85 ^{14}C yr (730 ± 100 cal yr BP; Hogg et al. 2013; Stuiver and Reimer 2018) from a basal peat overlying till between moraines M3 and M4, recognizing that the age was likely not a close limiting age. Although not inaccurate, the minimum-limiting age differs significantly from our reported age of 6,860 ± 140 yr for M3. This pattern of 'loose' constraining ages has been observed previously in the region, where minimum limiting ages for peat overlying till have been shown to greatly underestimate the true age of the landform. The assumption underlying the use of basal peat on glacial sediment is often that its development begins soon after a surface has been deglaciated, and that there have been no episodes of erosion or unfavorable climate that could strip initial growth and "reset" the date. The results from this study suggest that minimum ages obtained in this fashion must be treated with caution.

Although workers have studied the paleoglacial chronology of Patagonia for almost seventy years, prior studies have not revealed a pattern of progressively less-extensive Holocene glacier advances since late-glacial time, including in the early Holocene. We consider several reasons for the novelty of our finding:

a) Until recently, prior efforts could not directly date moraines and thus glacier expansions. The common assumption that radiocarbon-based minimum-limiting ages tightly constrain deglaciation in Patagonia. Many "late Holocene" moraines dated using this method may actually correspond to earlier times;
b) The few studies that obtained bracketing ages for glacial advances (close maximum, as well as minimum, ages of a glacial sequence) do show evidence for early Holocene glacier activity, although of uncertain extent (Mercer, 1965; Röthlisberger, 1986; Harrison et al., 2012; Strelin et al., 2014);
c) In areas studied previously, erosion may have partially to completely removed evidence of middle to early Holocene glacier advances, as appears to be the case in certain sites in New Zealand (Schaefer et al., 2009; Putnam et al., 2012);

Recent work has focused on outlet glaciers of the Patagonian Icefields, including recent efforts directly dating moraines using ^{10}Be (Kaplan et al., 2016). During the early Holocene, we infer that climate shifts favorable for glacier advance may have been relatively short; the South Patagonian Icefield and its associated outlet glaciers, although climatically sensitive (Strelin et al., 2014), may not have had enough time to respond (Jóhannesson et al., 1989) and leave a preserved geomorphic record on the landscape that was greater than subsequent expansions. That

is, in the early Holocene such cool periods occurred as brief excursions from what was still a generally warm period.

Fig. S1. Samples and geomorphology of the Torre Glacier area. a) Sample FRY16-02-03 (460 ± 20 yr BP) yields the youngest age in the region, from the granitic boulder (1.2 m x 1.0 m x 0.6 m) perched atop a quartz diorite block embedded in the sharp frontal ridge crest of M7. The Torre Glacier is in the background, behind Laguna Torre. b) Sample FR14-01-24 (6,910 ± 130 yr BP) is a granodiorite block perched on top of a sinuous ridge relatively free of vegetation, interpreted as the frontal moraine of M3. c) Sample FRY16-02-08 (6,920 ± 160 yr BP) was taken from an angular quartz diorite block on top of the outermost lateral of the M3 complex; this date is statistically indistinguishable from FR14-01-24. d) View to the northwest from the frontal ridge crest of M4. An inactive meltwater paleochannel is developed in the base of this moraine. Vegetation increases significantly on the leeward (right) side of this moraine, where a mature Nothofagus forest is encountered. M7 is the bare moraine ridge in the left background; the hummocky topography between M4 and M7 represents the dissected M5 and M6 advances.

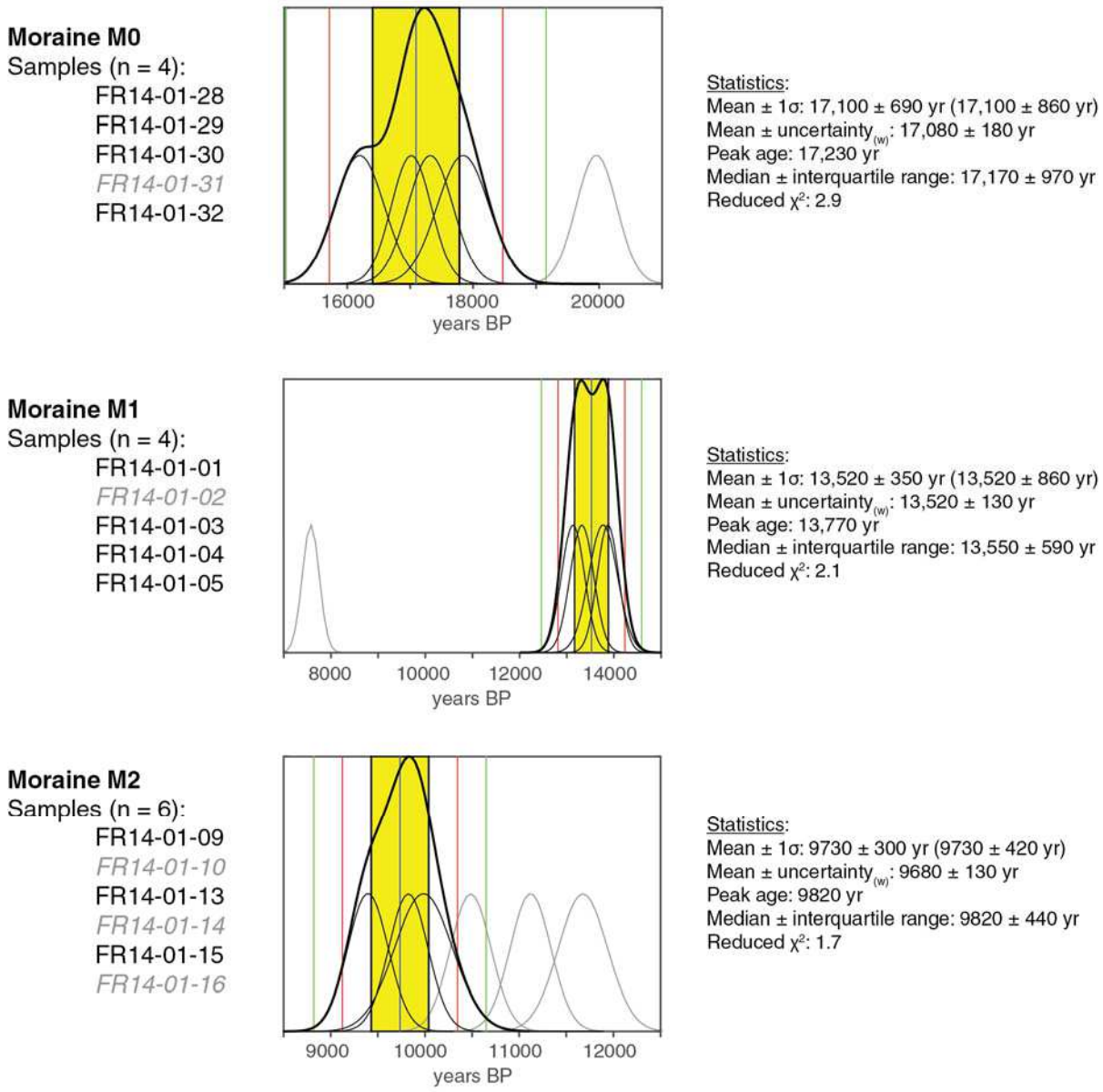

Fig. S2. Relative probability plots of moraine ages (thick curves) for M0, M1, and M2 moraines as the sum of the Gaussian probability density functions of individual dates (thin curves). Outliers are identified as samples that do not overlap with the mean at 2-sigma and are excluded from our analysis (gray curves, samples noted with gray italics). Blue central line represents the arithmetic mean value, and the parallel black, red, and green lines represent one, two, and three standard deviations from this value, respectively. The yellow band represents one standard deviation from the arithmetic mean. Moraine ages are reported as the arithmetic mean ± 1 sigma, but the population weighted means and medians of these moraines show good agreement and each could be used to represent moraine ages. We provide the reduced chi-squared statistic associated with each population; a value of <2 suggests analytical uncertainty alone is sufficient to explain observed variability (Bevington et al., 1993).

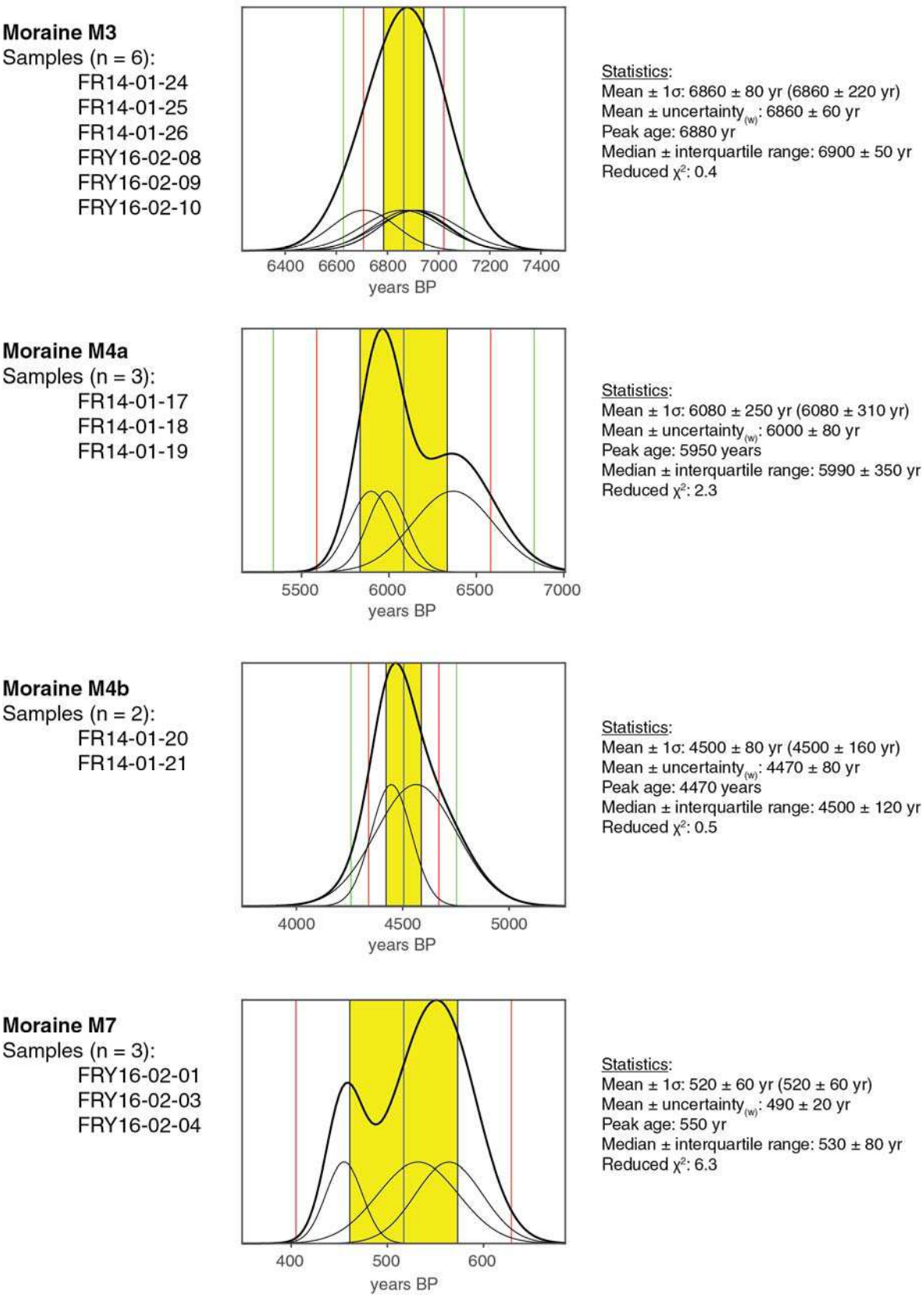

Fig. S3. Same as Fig. S2, but for moraines M3, M4a, M4b, and M7.

TABLES

Table S1. Age results

Sample	Lm v. 2.2.1	% uncertainty	v. 2.3. Lm	% of Lm v. 2.2.1	v. 3 Lm	% of Lm v. 2.2.1	v. 3 LSD	% of Lm v. 2.2.1
Moraine M0								
FR14-01-28	**16199 ± 395**	2.44%	15887	98.07%	15803	97.56%	15666	96.71%
FR14-01-29	**17843 ± 415**	2.33%	17489	98.02%	17365	97.32%	17198	96.39%
FR14-01-30	**17322 ± 361**	2.08%	16994	98.11%	16882	97.46%	16728	96.57%
FR14-01-31	***19958 ± 323***	*1.62%*	*19566*	*98.04%*	*19380*	*97.10%*	*19166*	*96.03%*
FR14-01-32	**17019 ± 318**	1.87%	16691	98.07%	16587	97.46%	16434	96.56%
M0 Average	**17100 ± 860**		16770	98.07%	16660	97.45%	16510	96.55%
Moraine M1								
FR14-01-01	**13873 ± 225**	1.62%	13609	98.10%	13595	98.00%	13527	97.51%
FR14-01-02	***7575 ± 178***	*2.35%*	*7410*	*97.82%*	*7473*	*98.65%*	*7479*	*98.73%*
FR14-01-03	**13771 ± 302**	2.19%	13507	98.08%	13494	97.99%	13436	97.57%
FR14-01-04	**13133 ± 244**	1.86%	12877	98.05%	12888	98.13%	12851	97.85%
FR14-01-05	**13322 ± 249**	1.87%	13058	98.02%	13061	98.04%	13019	97.73%
M1 Average	**13520 ± 540**		13260	98.06%	13260	98.04%	13210	97.66%
Moraine M2								
FR14-01-09	**9979 ± 306**	3.07%	9778	97.99%	9868	98.89%	9884	99.05%
FR14-01-10	***11109 ± 215***	*1.94%*	*10884*	*97.97%*	*10965*	*98.70%*	*10983*	*98.87%*
FR14-01-13	**9819 ± 208**	2.12%	9629	98.06%	9717	98.96%	9740	99.20%
FR14-01-14	***10477 ± 214***	*2.04%*	*10270*	*98.02%*	*10336*	*98.65%*	*10339*	*98.68%*
FR14-01-15	**9392 ± 176**	1.87%	9195	97.90%	9273	98.73%	9292	98.94%
FR14-01-16	***11662 ± 260***	*2.23%*	*11429*	*98.00%*	*11480*	*98.44%*	*11478*	*98.42%*
M2 Average	**9730 ± 420**		9530	97.99%	9620	98.86%	9640	99.06%
Moraine M3								
FR14-01-24	**6906 ± 133**	1.93%	6743	97.64%	6833	98.94%	6886	99.71%
FR14-01-25	**6709 ± 126**	1.88%	6551	97.64%	6646	99.06%	6709	100.00%
FR14-01-26	**6903 ± 130**	1.88%	6744	97.70%	6831	98.96%	6888	99.78%
FRY16-02-08	**6918 ± 158**	2.28%	6752	97.60%	6844	98.93%	6892	99.62%
FRY16-02-09	**6888 ± 142**	2.06%	6731	97.72%	6822	99.04%	6874	99.80%
FRY16-02-10	**6858 ± 156**	2.27%	6695	97.62%	6789	98.99%	6838	99.71%
M3 Average	**6860 ± 220**		6700	97.65%	6790	98.99%	6850	99.77%
Moraine M4a								
FR14-01-17	**5988 ± 111**	1.85%	5842	97.56%	5938	99.16%	6010	100.37%
FR14-01-18	**5897 ± 124**	2.10%	5754	97.58%	5842	99.07%	5916	100.32%
FR14-01-19	**6366 ± 231**	3.63%	6212	97.58%	6318	99.25%	6388	100.35%
M4a Average	**6080 ± 310**		5940	97.57%	6030	99.16%	6100	100.35%
Moraine M4b								
FR14-01-20	**4563 ± 190**	4.16%	4451	97.55%	4491	98.42%	4536	99.41%
FR14-01-21	**4446 ± 94**	2.11%	4337	97.55%	4375	98.40%	4416	99.33%
M4b Average	**4500 ± 160**		4390	97.55%	4400	98.41%	4480	99.37%
Moraine M7								
FRY16-02-01	**564 ± 35**	6.21%	532	94.33%	556	98.58%	570	101.06%
FRY16-02-03	**455 ± 19**	4.18%	424	93.19%	448	98.46%	469	103.08%
FRY16-02-04	**532 ± 42**	7.89%	501	94.17%	525	98.68%	541	101.69%
M7 Average	**520 ± 60**		490	93.94%	510	98.58%	530	101.87%

^{10}Be ages for Glaciar Torre samples, sorted by moraine, using the time-dependent Lal/Stone scaling model (Lal, 1991; Stone, 2000; Balco et al., 2008), the regional Patagonian production rate (Kaplan et al., 2011), and v. 2.2.1 of the constants file. Moraine average ages are presented as mean ages ± 1 standard deviation with the propagated 3% error of the Kaplan et al. (2011) production rated. We also present ages using the Lm scaling and the v. 2.3 calculator, the Lm

scaling and the v. 3 calculator, and the Lifton/Sato/Dunai “LSD” scaling (Lifton et al., 2014) and the v. 3 calculator. The percent difference in age between each alternative calculation and the v.2.2.1/Lm calculation is given in adjoining columns. The maximum difference between calculations is <4%; we conclude the choice of calculator does not fundamentally affect our conclusions.

References

Balco, G., Stone, J.O., Lifton, N.A., and Dunai, T.J., 2008, A complete and easily accessible means of calculating surface exposure ages or erosion rates from 10Be and 26Al measurements: Quaternary Geochronology, v. 3, p. 174–195, doi:10.1016/J.QUAGEO.2007.12.001.

Bevington, P.R., Robinson, D.K., and Bunce, G., 1993, Data Reduction and Error Analysis for the Physical Sciences, 2nd ed.: American Journal of Physics, v. 61, p. 766–767, doi:10.1119/1.17439.

Garibotti, I.A., and Villalba, R., 2009, Lichenometric dating using Rhizocarpon subgenus Rhizocarpon in the Patagonian Andes, Argentina: Quaternary Research, v. 71, p. 271–283, doi:10.1016/J.YQRES.2009.01.012.

Harrison, S., Glasser, N.F., Duller, G.A.T., and Jansson, K.N., 2012, Early and mid-Holocene age for the Tempanos moraines, Laguna San Rafael, Patagonian Chile: Quaternary Science Reviews, v. 31, p. 82–92, doi:10.1016/J.QUASCIREV.2011.10.015.

Hogg, A.G. et al., 2013, SHCal13 Southern Hemisphere Calibration, 0–50,000 Years cal BP: Radiocarbon, v. 55, p. 1889–1903, doi:DOI: 10.2458/azu_js_rc.55.16783.

Jóhannesson, T., Raymond, C.F., and Waddington, E.D., 1989, A Simple Method for Determining the Response Time of Glaciers, *in* Springer, Dordrecht, p. 343–352, doi:10.1007/978-94-015-7823-3_22.

Kaplan, M.R. et al., 2016, Patagonian and southern South Atlantic view of Holocene climate: Quaternary Science Reviews, v. 141, p. 112–125, doi:10.1016/j.quascirev.2016.03.014.

Kaplan, M.R., Strelin, J.A., Schaefer, J.M., Denton, G.H., Finkel, R.C., Schwartz, R., Putnam, A.E., Vandergoes, M.J., Goehring, B.M., and Travis, S.G., 2011, In-situ cosmogenic 10Be production rate at Lago Argentino, Patagonia: Implications for late-glacial climate chronology: Earth and Planetary Science Letters, v. 309, p. 21–32, doi:10.1016/J.EPSL.2011.06.018.

Lal, D., 1991, Cosmic ray labeling of erosion surfaces: in situ nuclide production rates and erosion models: Earth and Planetary Science Letters, v. 104, p. 424–439, doi:10.1016/0012-821X(91)90220-C.

Lifton, N., Sato, T., and Dunai, T.J., 2014, Scaling in situ cosmogenic nuclide production rates using analytical approximations to atmospheric cosmic-ray fluxes: Earth and Planetary Science Letters, v. 386, p. 149–160, doi:10.1016/J.EPSL.2013.10.052.

Masiokas, M.H., Luckman, B.H., Delgado, S., Skvarca, P., and Ripalta, A., 2009, Little Ice Age fluctuations of small glaciers in the Monte Fitz Roy and Lago del Desierto areas, south Patagonian Andes, Argentina: Palaeogeography, Palaeoclimatology, Palaeoecology, v. 281, p. 351–362, doi:10.1016/J.PALAEO.2007.10.031.

Mercer, J.H., 1965, Glacier Variations in Southern Patagonia: Geographical Review, v. 55, p. 390–413, doi:10.2307/213136.

Putnam, A.E., Schaefer, J.M., Denton, G.H., Barrell, D.J.A., Finkel, R.C., Andersen, B.G., Schwartz, R., Chinn, T.J.H., and Doughty, A.M., 2012, Regional climate control of glaciers

in New Zealand and Europe during the pre-industrial Holocene: Nature Geoscience, v. 5, p. 627, https://doi.org/10.1038/ngeo1548.

Röthlisberger, F., 1986, 1000 Jahre Gletschergeschichte der Erde: Salzburg, Verlag Sauerlander.

Schaefer, J.M. et al., 2009, High-frequency holocene glacier fluctuations in new zealand differ from the northern signature: Science, v. 324, p. 622–625, doi:10.1126/science.1169312.

Stone, J.O., 2000, Air pressure and cosmogenic isotope production: Journal of Geophysical Research: Solid Earth, v. 105, p. 23753–23759, doi:10.1029/2000JB900181.

Strelin, J.A., Kaplan, M.R., Vandergoes, M.J., Denton, G.H., and Schaefer, J.M., 2014, Holocene glacier history of the Lago Argentino basin, Southern Patagonian Icefield: Quaternary Science Reviews, v. 101, p. 124–145, doi:10.1016/j.quascirev.2014.06.026.

Stuiver, M., and Reimer, P.J., 2018, CALIB:, http://calib.org.